Biophysical Chemistry 25 (1986) 57–72
Elsevier

BPC 01090

CLOSED CHANNEL-OPEN CHANNEL EQUILIBRIUM OF THE SODIUM CHANNEL OF NERVE

SIMPLE MODELS OF MACROMOLECULAR EQUILIBRIA

Kenneth A. RUBINSON

* *The Five Oaks Research Institute, P.O. Box 507, Yellow Springs, OH 45387 and Department of Physiology and Biophysics, University of Cincinnati Medical Center, Cincinnati, OH 45267-0576, U.S.A.*

Received 6th December 1985
Revised manuscript received 29th May 1986
Accepted 15th July 1986

Key words: Transmembrane protein; Kinetics; Ordered system; Ionic equilibrium; Nernst equation; Sodium channel; Protein elasticity; Rubber elasticity; Young's modulus

The consistency of an electrodiffusion kinetics to describe the time-dependent opening of sodium channels of nerve suggests that motions over relatively long distances (on the atomic scale) are involved in the equilibrium as well. As a result, it is expected that a relatively large fraction of possible macromolecular conformations are unreactive. An equilibrium constant between locally reactive forms and the unreactive conformations is introduced. The consequences of this formalism is investigated in a square well potential, a harmonic potential, and a system consisting of two harmonic potentials with different spatial extents. The limits of knowledge from Nernstian behavior are shown. As an alternative to the Nernstian analysis, the experimental data of the sodium channel's quasi-equilibrium – the probability of the channel's being open as a function of voltage – can be described as resulting from motion caused by an electric field on a charge which is confined by a harmonic potential. A force constant is found from this analysis. (Such Hookian force constants cannot be found from spectroscopic experiments in condensed systems where the large-displacement vibrations are overdamped and, hence, spectroscopically unobservable.) From the force constant, an approximate value of the Young's modulus can be calculated. The modulus' value falls in the range for rubber. As for rubbers, the restoring force is, then, expected to be mostly entropic rather than enthalpic in origin. Using the appropriate theory for linear chains of rubber and the Young's modulus, the approximate length of the chain causing the rubber-like force is calculated. The result is found to be near the length suggested for the hydrophilic chains that connect transmembrane sections of the sodium channel.

1. Introduction

1.1. Background

Chemical kinetics in solution is not always adequately described by an activated state and concomitant changes in empirical quantities such as the enthalpies, entropies, volumes, and dipole moments of activation for the reaction. Since close proximity is a prerequisite for chemical interactions between atomic sites, if the molecular order among reacting units is retained for times longer than the reaction rate, a correct description includes a concentration distribution.

This basic idea has been applied to explain a wide range of chemical phenomena. Among them are rapid reactions [1,2] and radiation chemistry [3] in solution as well as triplet exciton recombination in solids [4,5]. Optical excitation transfers [6,7], electron transfers [8,9], and chemical reactions [10–13] of groups attached to oligomers and polymers have been modeled similarly. In essence, the conformation(s) in which a localized reaction

* Address for correspondence.

may take place are theoretically delineated from a continuum of conformations which are nonreactable.

Depending on the class of reactions, the sphere of reactable distance appears to vary in size. Electron transfer can occur across about 4 Å [8,9,14], while photon transfer can extend to much greater distances. When chemical bonding is involved, we can look to the distance along a 'reaction coordinate' from reactant to product [15]. Calculations for gas-phase molecular reactions indicate motions of distances less than 1 Å [16,17]. The work of Menger and his collaborators [18,19] and Scheiner [20] indicates the critical distance for reactions to be within a few tenths of an ångstrom of the van der Waal-contact distance.

In addition, in solutions, experimental evidence [21], theoretical considerations [22], and simulations [23] all indicate that translational motions of molecules consist of jump lengths in the range of 0.1 Å. All this evidence suggests that for reactions where bonds are made or broken and translational distances are greater than 1 Å, a concentration distribution may be required to characterize the reaction. A single or even multiple activated state may be insufficient.

This is especially true when a reaction occurs in a membrane with the effects of a relatively high viscosity. While the continual solvent collisions ensure thermal equilibration, they also damp the motions. In the limit of strong coupling to the solvent, the low-energy, large-displacement vibrations are overdamped [24]. The motions, including configurational changes, become diffusion-controlled. This point is made with clarity in a classic paper of Kramers [25]. For polymers, where inevitably a distribution of diffusional relaxation times are found, the factors involved are covered in detail by Doi [26].

A further point is germane to the continuum of biopolymer conformations where only small activation energies (less than a few kT) can separate them. A deeper investigation of kinetics exposes significant problems connecting statistical descriptions with the empirical kinetics. This point is clearly expounded by Boyd [27]. As noted by Widom [28,29] in work that derives from Zwolinski and Eyring [30] and Rice [31], specific chemical species only become relatable to statistical states when the activation energy between the species is relatively large. This difficulty – investigated in gas-phase reactions – brings into question some possible problems in defining various 'states' in globular proteins where a large number of slightly different configurations might exist within a narrow energy range.

For the sodium-channel kinetics, often in the past, in order to match the time dependence of a voltage-clamp current or the total noise-frequency spectrum, models with numerous elementary reaction steps have been used (e.g., refs. 32–35). The author has proposed a scheme which includes simultaneous thermal and electrodiffusion [36–38]. Multi-state schemes can be chosen to approximate well the Nernst-Planck electrodiffusion behavior (ref. 39 and author's unpublished work) or vice versa. However, the kinetic parameters' dependence on applied potential [40,41] can be used to decide whether a model at least agrees with possible kinetic behavior.

When chemical reactions are controlled by electrodiffusion, the rate is linearly dependent on field (fixed charge, fixed distance). Rate constants reflecting activation-state-controlled reactions perturbed by the applied field exhibit logarithmic dependence on the field. Using such criteria, unacceptable models can be discarded while narrowing the range of the correct approximations. The judgement is, thus, linked to the realm of descriptive chemistry. On this basis, the electrodiffusion model is consistent with other, known, chemistry.

This diffusion/activation dichotomy of interpretive kinetics in essence reproduces similar arguments about models of liquid-state diffusion [42]. The diffusion can be interpreted as either being due to molecular jumping into relatively large holes (activation controlled) or through a large number of small, random hops. The temperature dependence of the former is assumed due mostly to enthalpic effects. For smaller jumps, temperature effects are argued to be due to changes in the free volume.

For relatively highly structured systems such as the sodium channel an associated question is how the measured equilibrium behavior is related to the rate constants. This question is the subject of

the present work. For instance, consider a large protein or subunit which can distort or shift position by a small percentage of the protein's diameter. An example of such structural changes in the gap junction has been observed by Unwin and Ennis [43]. For example, assume a 50-Å-diameter protein where a change in structure distorts one binding site position by 1 Å. This is only 2% of the protein's diameter (The displacement of a single-quantum diatomic vibration is about 2% of the bond length; e.g., HCl.) However, the distance of motion is such that a substrate, bound through a number of noncovalent bonds, might become 'unbound' due to the change in total binding energy relative to solvent molecules [18–20].

1.2. The field-dependent sodium channel as a test case

The sodium channel is exceptionally well suited for investigating the relationships between macromolecular conformational equilibria and kinetics involving bond formation. One benefit is that both the open-closed equilibrium and rates change with applied potential and are independently measurable. In addition, from the voltage dependence of the rates, the individual reactions involved can be classified by behavior of rate constants with potential [41].

Other benefits compared to measurements made in free solution are listed below.

(a) The rates and equilibrium can be manipulated by an easily changed electric field.

(b) The highest electric fields are larger than are generated in chemical voltage-jump apparatus used for chemical studies in liquids.

(c) Significant problems associated with unwanted effects at electrode surfaces at high potentials (e.g., charge injection and mechanical distortion [44]) are probably absent.

(d) The glycoprotein's [45] structure is spatially ordered [46,47]. This eliminates the problems due to having molecules oriented randomly over 4π steradians. In addition, anchoring in the membrane allows effects due to simultaneous molecular translations and conformational changes to be separated from those of molecular rotations.

(e) The sodium channels' selectivity for sodium allows data to be obtained from a single molecular species in the presence of 'impurities'. Further, noise analysis allows measurements to be made on a solitary channel.

(f) In essence, the electrochemical potential due to Na^+ allows amplification of the information that the molecules have arrived at the conducting form.

(g) The 'product' of the reaction is an ionic current. Thus, electrochemical methods allow greater sensitivity than any other assay method that can be done in real time.

(h) The time course of the changes is relatively slow – in the millisecond range [36,38,48]. Thus, details of the kinetics are more accessible than the usual solution reactions.

(i) The polymer appears to be monodisperse [48].

The drawbacks to the use of the sodium channel – compared to utilizing a solution or liquid-crystal species – are due to the presence of an extra, membrane, phase which may introduce the following ambiguities:

(A) The local dielectric constant(s) and exact location(s) of the potential drop(s) are open to surmise;

(B) The exact average or local environmental viscosity is unknown;

(C) Due to unknown dielectric constants, unknown partitioning, and/or other interface effects, the local ionic concentrations and their effects are widely hypothetical.

The sodium-channel open/closed probability can be described by at least two general equilibrium models. These reflect the origins of the two curves which are used to fit the data of P_{open} vs. potential (fig. 6) – a complementary error function and a Nernstian equilibrium equation. As described below, the variables of the complementary error function are attributable to elastically bound charges moving across at least part of the applied potential. Through this model, analysis of the data leads to the conclusion that the macromolecule's mechanical properties are rubber-like. The second, Nernstian curve, is shown to be ambiguous in its chemical implications. Before these two models are elucidated, a simplified example is presented to illustrate the ideas of divid-

ing biomacromolecular configurations between a locally reactable one and the range of non-reactable forms.

2. A square well confinement of unbound charges

The first model presented describes the equilibrium of a set of ions confined in a square well potential. It is not an analogue of the sodium channel since the expected voltage dependence of the equilibrium does not fit the experimental data. However, it does provide a straightforward illustration of the principal features of an equilibrium involving a continuum. As illustrated in fig. 1, the ordinate of the graph is used to plot the internal energy and/or the density of states along the x-axis. The x-axis is normal to the membrane surfaces. The model is classical and does not include fluctuations or tunneling.

The distance between the infinite barriers is $\bar{d}$. The charges are free to move within the well. The dashed line to the right indicates the boundary of reactable and nonreactable regions. The separating line's location is called p, which is a fraction of $\bar{d}$. In fig. 1, $p = 0.8$.

Only the fraction of the charges residing in the local regions can react further in what appears to be a single reaction step. The boundary's position depends on the viscosity and the characteristic time for observation of the reaction. The fraction of local region increases with lower effective viscosities and longer characteristic times.

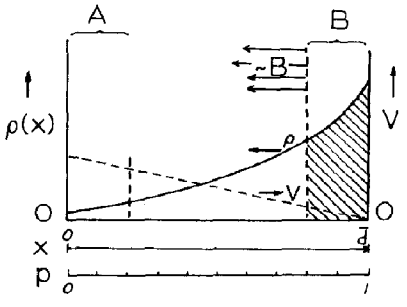

Fig. 1. Nomenclature for discussing the distribution of free cations retained in a square well potential. The locally reactive form is labeled B, the locally nonreactive form is the material in the configuration ~ B.

For the square well, there are two different cases which should be considered. One is where only form B is observable by experiment. In that case, the remainder of the continuum will be labeled 'not B', i.e., ~ B. The sodium channel is of this type. The other case occurs when the states at both extrema of the continuum are observable: form A as well as form B. In this latter case, there are two boundaries. Given the B/~ B boundary is at $p_B = 0.8$, the boundary for 'form A' is (assuming symmetry) at $p_A = 0.2$ – the dashed line at the left.

The experimentally determined equilibrium constants of such an extended system must be calculated from the populations in the applicable regions of the continuum. It is usually assumed that [B]/[A] = [B]/[~ B]. However, this is true only in the limiting case when $p = 0.5$. In the remainder of this section, the limitations of the two-state equilibrium constant are illustrated. The different equilibrium constants are annotated with subscripts. When the equilibrium constant is described by the concentrations of two locally reactable forms it is labeled K_t – i.e.,

$$K_t = [B]/[A]. \quad (1)$$

When only [B] is observable, the equilibrium constant is labeled K_∞:

$$K_\infty = [B]/[\sim B]. \quad (2)$$

The equilibrium populations along the continuum from which [A], [B] and [~ B] are calculated are determined by the total energies along the continuum and the applicable Boltzmann distribution.

The following assumptions are made:

(1) The movable charges are positively charged. Any motions of negatively charged species are included as positive charges moving in the opposite sense.

(2) The charges are retained mechanically within the slab (square well).

(3) Excluding the applied potential, within the square well, the environment is homogeneous both along the x-axis and normal to it.

(4) Boltzmann statistics applies to the system.

(5) For convenience, the number of charges is fixed and the number density normalized to unity.

(6) Any change in the entropy due to electric-field-induced demixing can be ignored. In other words, the entire free energy change resides in the potential energy.

(7) The degeneracy of each state within the continuum is the same – unity. If the states represent configurations of a macromolecule, we might expect the energies of configurations in the middle spatial region to have somewhat greater degeneracies than those at the extremes. However, the simplifying assumption is used in the absence of a basis for assigning degeneracies.

(8) The field at all locations across the slab is constant; the potential drop is linear.

Concerning this last point: if the positions of the charged species did affect the potential, then the ion distribution would be equivalent to that calculated by Gouy-Chapman theory. However the distribution would be truncated at the far boundary if $\bar{d}$ is short enough.

2.1. *State energies and populations: two-state and continuous distributions*

There are a number of differences between the continuum system and a two-state description of the equilibrium for the square well. These are presented next for the case where $p = 0.9$ and for a number of different voltages as illustrated in fig. 2. For fig. 2 as in fig. 1, the population distribution is plotted together with the energies for a number of voltages applied between A and B.

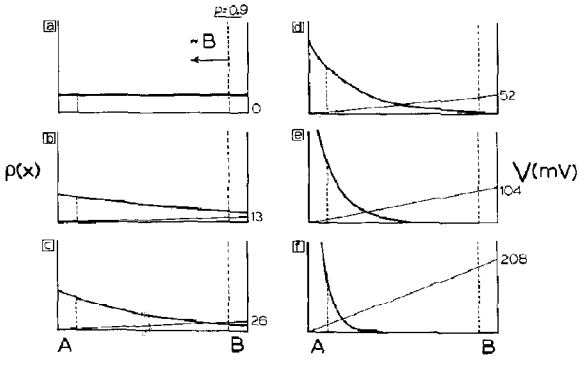

Fig. 2. Distributions of $z = +2$ charges under the influence of various voltages (in mV) at 6 °C.

Those shown are for ions of charge +2.

If the voltage is zero, then all the energies of the continuum are equal and $E_A = E_B$ as shown in fig. 2a. When $p = 0.9$,

$$K_t = [B]/[A] = 1;\ p = 0.9 \tag{3}$$

and, when only the quantity [B] can be detected,

$$K_\infty = [B]/[\sim B] = [0.1]/[0.9] = 0.111;\ p = 0.9. \tag{4}$$

As is derived in appendix A, for a general value of p, the continuum-state equilibrium constant is given by

$$K_{\infty,p} = \frac{e^{\zeta} - e^{p\zeta}}{e^{p} - 1} \tag{5}$$

where $\zeta = -\Delta V \cdot z\mathcal{F}/RT = -\Delta V z/0.0239$ at 5 °C. Recall, Nernstian behavior is described by

$$K = \exp(\zeta) \tag{6}$$

In section 2.2, the differences in behavior between the usual two-state equilibrium constant and the continuum equilibrium constant (eqs. 1 and 2, respectively) for the square well potential are described.

2.2. K_∞ *as a function of* ΔV *and* p*: special and limiting cases*

Fig. 3 shows the values of K_∞ with various values of p for the case where $z = +2$. The dashed line plots the Nernstian behavior. All the K_∞ curves are nonlinear except when $p = 0.5$. In that case, the slope is half the logarithmic Nernstian rate – appearing as if $z = +1$. Mathematically, the behavior with $p = 0.5$ is easily shown.

$$K_\infty = \frac{e^{\zeta} - e^{\zeta/2}}{e^{\zeta/2} - 1} = \frac{e^{\zeta/2}(e^{\zeta/2} - 1)}{e^{\zeta/2} - 1} = e^{\zeta/2};\ p = 0.5 \tag{7}$$

The reason the apparent charge is half of the actual charge value is that at zero potential, half of the charge is distributed on the opposite side of the $p = 0.5$ demarcation and, thus, only half the total charge is transferred. As can be seen from the equality of the slopes in fig. 3 at potentials

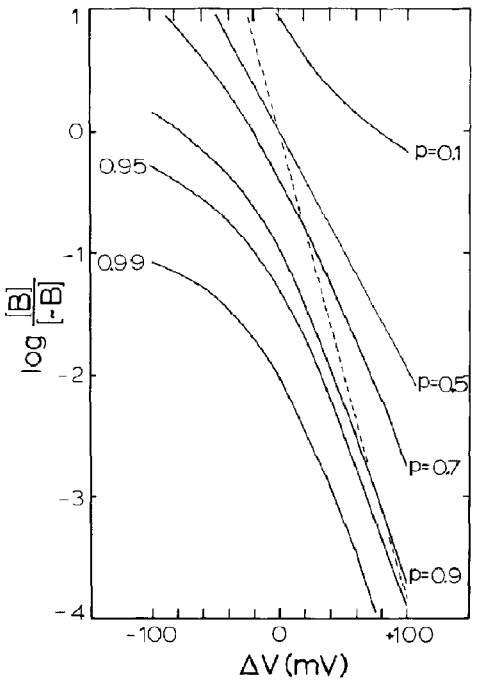

Fig. 3. A plot of log K_∞ vs. potential for various values of p, the fractional distance of locally reactive forms, for free $z = +2$ ions constrained in a square well potential. At $p = 0.5$, the dividing line is at the central point of the well.

above about 60 mV, the charge appears to equal z for the square well system only when the voltage is relatively large, and the system is nearly completely polarized.

Two general ways exist for p to become 0.5, and for the Nernstian behavior to appear. One is for the total distance $\bar{d}$ to decrease with a fixed length of reactive region. The other occurs when the reactive regions expand with fixed $\bar{d}$. This latter effect occurs in the limit of longer time. In both cases the two local regions eventually converge along a $p = 0.5$ division and Nernstian behavior ensues. In other words, Nernstian behavior is always obtained in the limit of short distances between conformations A and B or in the limit of long time. Thus, the continuum equilibrium passes smoothly into behavior described by a two-state system. Another way to consider this point is that all the material 'lost' in the nonreactable range becomes locally reactable.

There is one final point worth mentioning concerning the relationship of the equilibrium and rate constants. The continuum equilibrium constant for this square well system may in some cases appear to behave similarly to those for simple two-state equilibria. Nevertheless, the close relationship of the equilibrium and rate constants does not hold:

$$K_\infty \neq k_f/k_r \tag{8}$$

where k_f and k_r are the first-order rate constants expected for the system in the limit of short distances or long times.

2.3. K_t as a function of p

If both [A] and [B] can be measured, and the two boundaries are equally placed from the extremes, then the value of K_t will appear to be Nernstian in its behavior but with a reduced effective charge of pz. * Thus, if p – the relative local distance – changes, the charge of the species involved will appear to change. The reason for this variation is that different fractions of the continuum states are lost between the demarcations p and $1 - p$.

From an observer's point of view, an alternate and incorrect interpretation of the charge in K_t with p might be made. One might suggest, incorrectly, that there is a reduction of the fraction of the voltage traversed by the ion even though it continues to cross the entire applied voltage.

3. Elastically bound charges in an external field

3.1. The potential

In this model we consider that an ionic charge is constrained elastically in a potential which is quadratic with the charge's displacement from an equilibrium origin (see fig. 4). The potential is

* This can be derived by a calculation similar to eq. A5 of the appendix.

$$[B]/[A] = \left(\int_p^1 e^{m\xi}\,dm\right) \Big/ \left(\int_0^{1-p} e^{m\xi}\,dm\right)$$

oriented in an ordered matrix with its x-axis fixed as shown in the figure. A simple mechanical analogy is a charged body connected by a Hooke's Law spring to a large mass. Note that the parabolic potential arises from a mechanical constraint – independent of the electric charge. The model is an analog for a charged region of a protein being restrained by an elastic connection with the rest of the mass. As was done for the square well, we again assume that the field is independent of the positions of the charged groups.

The total potential felt by the charges consists of the superposition of the quadratic mechanical potential with an electrostatic potential from interaction between the ionic charge and the external field. The properties of the ionically charged-elastically constrained body under the dual influences are demonstrated below.

The linear potential is given by

$$U_l = z(V/\bar{d})(x - A) \tag{9}$$

where z is the ionic charge. The potential V is more precisely delineated by

$$V/\bar{d} = \left(V_{app}/\bar{d}\cdot\epsilon\right) = E \tag{10}$$

where ϵ is the effective dielectric constant and E the associated assumed-linear electric field. In the equations below, E is substituted for $V_{app}/\bar{d}\epsilon$. Eq. 9 becomes

$$U_l = zE(x - A) \tag{9}$$

The unperturbed quadratic well is described by

$$U_{quad} = \tfrac{1}{2}K(x - x_o)^2 + U_o \tag{11}$$

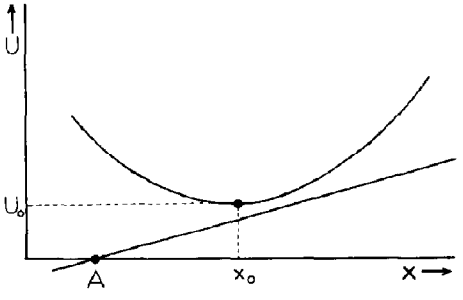

Fig. 4. Nomenclature for discussing the influence of a constant electric field on ions constrained by a Hookian potential.

where K is the force constant for a Hooke's Law spring. The sum of U_l and U_{quad} is

$$U = \tfrac{1}{2}K(x - x_o)^2 - zE(x - A) + U_o$$

or

$$U - U_o = \tfrac{1}{2}K(x - x_o)^2 - zE(x - A) \tag{12}$$

After completing the squares and rearranging, eq. 12 yields

$$U - \left[U_o + zE(x_o - A) - z^2E^2/2K\right] = \tfrac{1}{2}K\left[x - (x_o - zE/K)\right]^2 \tag{13}$$

Therefore, in the presence of the external voltage (subscript f), the sum potential consists of a congruent parabola with

$$x_{of} = x_o - zE/K \tag{14}$$

and

$$U_{of} = U_o + zE(x_o - A) - z^2E^2/2K \tag{15}$$

The shift of the minimum point of the parabolic potential under the influence of the voltage is quantified by

$$x_{of} - x_o = -zE/K \tag{14}$$

and

$$U_{of} - U_o = -\left(z^2E^2/2K\right) + zE(x_o - A) \tag{15}$$

As seen from eq. 14, the spatial shift of the congruent parabolic potential depends directly on z and E and inversely on the force constant. The magnitude of the shift is independent of the value of x. Meanwhile, eq. 15 shows that the minimum of the potential energy is shifted by an amount which is a complex function of the charge, voltage, force constant, and spatial position.

3.2. The mass distribution created by the potential

It is assumed that the charged, elastically bound groups follow Boltzmann statistics. Therefore, in a parabolic potential well with $x_o = 0$ and $U_o = 0$, the normalized mass distribution will be given by

$$\rho(x) = (2\pi kT/K)^{-1/2}\exp\left[-\tfrac{1}{2}Kx^2/kT\right] \tag{16}$$

– describable by a Gaussian curve. The width of the distribution depends on the ratio of the curvature of the quadratic potential and the thermal energy. The curvature depends on the force constant.

When the external voltage is changed, the whole distribution simply shifts position. However, the shape of the potential remains congruent as seen in eqs. 11 and 13. So does the width of the Gaussian spatial distribution as it changes its position.

We now consider what fraction of the area of the curve appears to the right of the perpendicular line in fig. 5. The line delineates the nonreactable area to the left from the locally reactable region to the right. As the potential changes, the Gaussian distribution is shifted to the right an amount directly proportional to the voltage. As a result, the fraction of material in the local conformation is described by a complementary error function. As shown in appendix B, $\rho(x)$ is related to the areas under the Gaussian curve by

$$\int_y^\infty \rho(x) = \tfrac{1}{2}\mathrm{erfc}\left[y/\sqrt{2(kT/K)} \right]. \tag{17}$$

The integral limit y is linearly related to the position of the parabola along the x-axis and, hence, to the fraction of the distribution which is locally reactable. To fit the experimental data, y must be associated with the voltage. Doing so allows the force constant, K, to be calculated

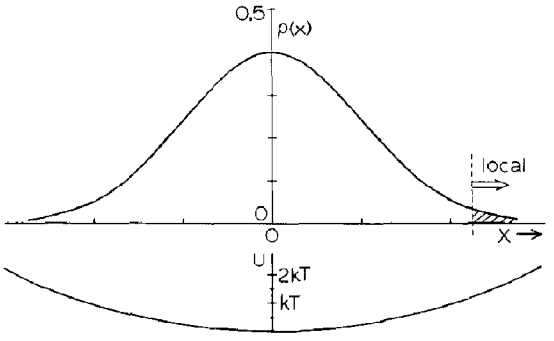

Fig. 5. (Bottom) The harmonic potential in energy units of kT. (Top) The accompanying distribution of mass. The local-nonlocal boundary is fixed while the material translates under the influence of an external field.

from the experimental curves' best-fitting erfc. The needed relationship is found in eq. 14. When the origin of the parabola coincides with the dividing line, then $E = E_{P=0.5}$, and we can let $x_0 = 0$. Then we can identify changes in y as being equal to $-z(E - E_{P=0.5})/K$ through eq. 14. Therefore,

$$\int_{-|z|E/K}^\infty \rho(x) = \tfrac{1}{2}\mathrm{erfc}\left[-\left(|z|/\sqrt{2KkT} \right)(1/\bar{d})(V - V_{P=0.5}) \right] \tag{18}$$

where a substitution $E = (1/\bar{d})V$, such as noted in eq. 10, has been made on the right-hand side. The usual assumptions that the entire potential is effective and $\epsilon = 1$ are made.

The P_{open} data have been fitted with the function

$$P_{\mathrm{open}} = \tfrac{1}{2}\mathrm{erfc}\left[\mathrm{factor} \cdot (V - V_{P=0.5}) \right] \tag{19}$$

Thus, by comparing eqs. 18 and 19, the prevoltage factor of the complementary error function is found.

$$\mathrm{factor} = -\left(|z|/\sqrt{2KkT} \right)(1/\bar{d}) \tag{20}$$

The value of $|z|$ may be approximated, but in the case of the voltage-clamped sodium channels it can be determined from the kinetic analysis. An effective value of $|z|$ has been found under precisely the conditions needed; it accounts for the value of ϵ and the fraction of the applied voltage which affects the system. Together with the prevoltage term determined by fitting the P_{open} data with eq. 19, the value of K may be calculated within an approximation of $\bar{d}$. $\bar{d}$ is assumed to be 10 Å to ensure being correct within a single order of magnitude. If $|z|$ is not known, K may be approximated using $|z| \approx 4$ net elementary charges.

The results of such an analysis are listed in table 1. Data of P_{open} found from the voltage-clamp data described in the previous paper [38] and from the noise-analysis data of Moczydlowski et al. [48] are included. The force constants from the latter are approximated assuming $z = 4$ and the curve fits are shown in fig. 6. It should be noted that the above analysis will hold even if the

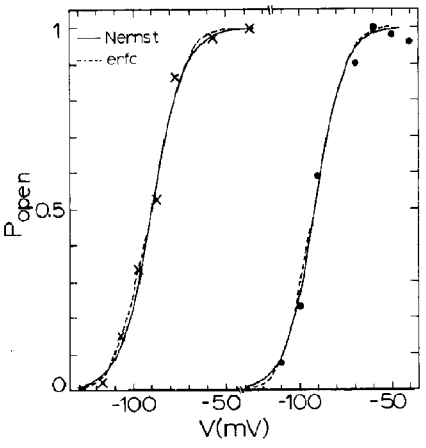

Fig. 6. Data and best fitting curves for P_{open} data measured by noise analysis of sodium channels. The data are from Moczydlowski et al. [45]. Note the split in the voltage axis. The values for best fit are: (×) Nernst −2.8 charges with $P_{0.5} = -90$ mV, erfc factor 47 with $P_{0.5} = -90$ mV; (○) Nernst −3.1 charges with $P_{0.5} = -92$ mV, erfc factor 52 with $P_{0.5} = -92$ mV.

motion of the charges and the mechanical potential have components perpendicular to the direction of the field. Some possible molecular mechanisms for such motions are noted by Frohlich [49].

3.3. Comment on the derived force constants

Using the harmonic-potential model, the force constants calculated from the P_{open} data lie in the range around 20 dyn cm^{-1}. In table 2 This value is compared with representative force constants for stretching and distortion of various types of chemical bonds. The magnitudes of the force constants determined here are without precedent. It is worth noting that this force constant is found from an overdamped system and is not accessible through a harmonic perturbation.

It might be possible that the motion of a charge at one end of a relatively long molecular arm retarded only by a single weak dihedral distortion force at the opposite end could produce an apparent K value in the right range. In addition, stretching a chain consisting of a number of dihedrally distortable bonds could also produce such a value. However, a relatively free rotation about the bonds should ensue before the chain extension will be limited by dihedral distortion forces. The preferential onset of the chain's free rotation is due to the low activation energies (generally less than 1000 cm$^{-1} = 5kT$) for bond rotation [50,51].

As a result, the harmonic potential of the model, as illustrated in figs. 4 and 5, may not be due to enthalpy effects at all. To carry this argument further and relate the result to descriptive chem-

Table 1

Force constants calculated from erfc fits to the data

Experiment	z [a]	Pre-voltage factor [b]	K(calc) (dyn cm^{-1}) [c]
Paper I(A)	$3._5$	$44._5$	20
Paper I(C)	$5._1$	$70._9$	17
Fig. 6(×)	(4)	47	23
Fig. 6(○)	(4)	52	19

[a] Calculated from kinetics or ( ) indicate approximate value.

[b] The pre-voltage factor has a value: factor = $(|z|/\sqrt{2kTK})(1/\bar{d})$. The value of $\bar{d}$ is assumed equal to 10^{-7} cm. The following values are used to calculate K: $k = 1.380 \times 10^{-16}$ erg degree^{-1}, $T = 285$ K, V_{eff} = total potential, $\epsilon = 1$. Since 1 eV = 1.602×10^{-12} erg, then with substitutions and assumptions: $K = (57.1 \cdot z/\text{factor})^2$, where the factor is found from the least-squares fit to the data.

[c] 1 dyn cm$^{-1} = 10^{-5}$ mdyn Å$^{-1} = 10^{-3}$ N m^{-1}.

Table 2

Representative force constants

Identification	Force constant *	References
Single-bond stretch	5–8	a, b
Single-bond bend	1	a, b, c
Hydrogen-bond stretch	0.3	d, e
Hydrogen-bond bend	0.03	d, e
Single-bond torsion	0.02	b, c
Sodium channel model	0.0002	this work

* Units are: (for stretching) value $\times 10^{+5}$ dyn cm^{-1} or × mdyn Å^{-1}; (for bending and torsion) value $\times 10^{+16}$ dyn cm rad^{-2} or × mdyn Å rad^{-2}.

[a] R.M. Silverstein, G.C. Bassler and T.C. Morrill, Spectrometric identification of organic compounds, 3rd edn. (Wiley, New York, 1974) ch. III.

[b] J.H. Schachtschneider and R.G. Snyder, Spectrochim. Acta 19 (1963) 117, especially table 4.

[c] D.W. Scott and M.Z. El-Sabban, J. Mol. Spectrosc. 30 (1969) 317.

[d] S.G.W. Ginn and J.L. Wood, Spectrochim. Acta 23A (1967) 611.

[e] T. Miyazawa and K.S. Pitzer, J. Am. Chem. Soc. 81 (1959) 74.

istry, it is worthwhile to find the Young's modulus equivalent to the force constants calculated from the data. This calculation is done next.

3.4. Young's modulus equivalent to K for a polypeptide chain

The Young's modulus of a bulk material relates the relative extension of a material to the tension placed on it. For a homogeneous substance of length l_o and cross-section $\mathscr{A}$ which is elongated by Δl due to a force, F_n, normal to the cross-section, the Young's modulus, E is given by

$$(\Delta l/l_o)E = F_n/\mathscr{A}. \tag{21}$$

For small Δl values the modulus is independent of the elongation; it is a Hooke's Law body [52]. The force on a Hooke's Law body, $F_n = K(l - l_o)$, and

$$K = \mathrm{d}F_n/\mathrm{d}l. \tag{22}$$

Therefore,

$$K = \mathrm{d}F_n/\mathrm{d}l = E\mathscr{A}/l_o \tag{23}$$

For any single peptide chain, $\mathscr{A} \approx 30$ Å^2, and we assume that $l_o \approx 10$ Å. Therefore, a force constant of 18 dyn cm^{-1} (see table 1), is equivalent to

$$E \approx 6 \times 10^8 \text{ dyn cm}^{-2}.$$

Because of the assumptions necessary, the modulus is expected to be correct only within an order of magnitude.

For comparison, values of Young's modulus range from approx. 1×10^{11} for metallic lead to about 20×10^{11} dyn cm^{-1} for steel. However, rubber has a modulus in the range 10^6–10^7 dyn cm^{-2} [53,54]. The calculated value of Young's modulus may also be compared to that measured for bulk proteins. For example, Muller and Ferry [55] found that films composed of 12–20% fibrin possess moduli in the range 0.4×10^6–5×10^6 dyn cm^{-2}.

The force constants listed in table 1 derive from the open-channel probabilities found from both standard voltage-clamping experiments and noise analysis. The conformational change associated with channel opening/closing is described here in a general way: as a charged region of a macromolecule moving under the influence of the applied field and confined elastically by interconnection with other masses. If this general interpretation of the experimental data is correct, the mechanical properties within the sodium channel can be characterized as rubber-like and similar to some other protein structures.

3.5. Young's modulus and chain length

The value of the Young's modulus can be related to the molecular weight of the polymer chain that produced it. The polymer is considered to consist of N_0 molecules making up a cylinder that has length l_o when undeformed and l when deformed. For the case where a single molecular chain consists of units that freely rotate about the single bonds contained in it and that is pulled only at the two ends

$$E \approx 3RT\rho(1/M) \tag{24}$$

where E is Young's modulus, $R = 8.314 \times 10^7$ dyn cm^{-2} K^{-1} mol^{-1}, T is the temperature (300 K), ρ the density of the material (assumed unity), and M the molecular weight of the chain. This equation has its origin in the work of Kuhn [56] which had an incorrect factor in it. The arguments were restated by Wall [57]. The basis of the equation and the problems in its derivation are clarified by Treloar [58]. Eq. 24 holds for small values of the extension, $\Delta l = l - l_o$, and a purely entropic origin for the elasticity.

Inserting the value of $E = 6 \times 10^8$ dyn cm^{-1}, the molecular weight of the chain is found. Here $M \approx 120$ a.m.u. Since the chain alone is about one-half of the polypeptide, this suggests a tripeptide chain to be responsible. This is the same order of length * as the acidic segments of the sodium channel (4–17 amino acids) which are assigned to the cytoplasmic side of the membrane

* If there are a number of connecting chains, under (quasi)equilibrium conditions, the spring with the largest force constant would be the last to yield in the channel opening and the first to produce an effect in the channel's closing. In other words, the shortest chain is expected to produce the representative force constant observed.

as determined by Noda et al. [47] by inference from the nucleotide base sequence. It is suggested that these acidic segments join together adjacent transmembrane structures of the channel.

It may be that the acidic segments do, indeed, act as the origin of a restoring force. They might either pull the transmembrane segments of the channel together or push them apart. Such a structure-function relationship also suggests how proteases applied internally might cause their effects on the sodium channel [59,60]. If the proteases cut the acidic residue chains, the spring-like action which causes the channel closure would be destroyed, and the channel would not close by itself. This is the behavior observed [59,60].

The above hypothesis may be the result of a coincidence. However, the low restoring force of the charged subunit(s) probably precludes the presence of a larger number of atomic contact points between the subunit(s) and other proximate masses. This mechanism suggests why the channel is so sensitive to the proteases and other perturbants which produce similar effects and the channel's sensitivity to denaturation [61].

4. The general case of two harmonic potentials

The purpose of this section is two-fold. First is to show why a relatively sharp boundary between locally reactable and nonreactable conformations can be used. Second is to show the limitations of the molecular information obtainable from the Nernstian analysis applied to the P_{open} vs. voltage data for the sodium channel.

The square well analysis developed in section 2 suggests that unbound, confined charges exhibit Nernstian behavior only when the characteristic time for the reaction is long enough to allow the reactable regions to include the entire conformational range. The entire continuum is then divided in the middle into the two chemical species.

It is more correct to represent each of the two species within its own (nearly) harmonic potential. Each occupies a number of energy states within the potential. The multidimensional harmonic potentials may originate from interactions associated with bond stretching, bond bending, van der Waals forces, electrostatic interactions, etc. Nevertheless, each dimension of the potentials is approximately equal in extent. (An analysis toward a different end of two intersecting parabolic energy functions with slightly different widths has been made by Koeppl and Kresge [62]).

Alternatively, the potential may be entropic in origin such as that giving rise to rubber elasticity. To account for this possibility, in this section are analyzed descriptions which include the two harmonic potentials associated with the reaction coordinate. Unlike the usual chemical models, however, the potentials are allowed to extend over different lengths. This is done in the same spirit as delineating a shorter, locally reactable region from a broader, nonreactable region. In addition, as will be shown here, the spatial shift described in section 3 arises naturally in the two-well system but only when the widths of the two wells are significantly different.

The entropy of charge mixing/demixing is ignored, and anharmonicities in the potentials will not be considered. Another assumption which is usually made requires the ionic charge to remain constant as it passes between the two potential wells. Implicitly or explicitly, such assumptions are an integral part of, e.g., interfacial electrochemistry [63–65]. This latter assumption is not made here.

The inequalities in the widths of the potentials are introduced to account for uncertainties regarding the spatial extent over which a 'species' is defined for equilibria involving macromolecules. For instance, the charged portion of a macromolecule may be restrained only by weak forces while, once in the reactive conformation, a relatively strong, short-range interaction may define the reactable species. Such a set of potentials is illustrated in fig. 7. The potentials are characterized by the following: their force constants, K'' and K'; their energy minima U_o'' and U_o'; and the spatial positions of the minima x_o'' and x_o', respectively, for the double primed ($''$) and primed ($'$) species. When the two potential wells have different acuities, the wider one will be labeled ($'$). This means that $K' < \text{or} \ll K''$. Having $K'' = K'$ means that the two wells are congruent in shape.

The applied potential V remains zero at point

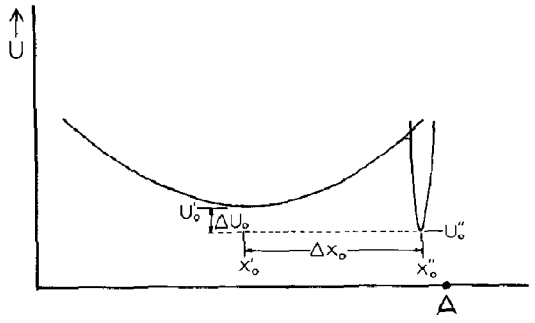

Fig. 7. Nomenclature associated with a two-well potential in the presence of an external voltage with a zero value at point A.

A. V is understood to represent (V_{eff}/ϵ) where V_{eff} is the fraction of the applied voltage which appears across the distance $\bar{d}$. For clarity, substitution of E as in eq. 10 is not done in the following equations.

We assume that the vibrational zero-point energies are vanishingly small on this scale and that the allowed energies within the potentials form a continuum. The membrane and dielectric effects are accounted by the simplest model: the voltage results in a linear electric field over a distance $\bar{d}$.

As illustrated in fig. 7, two additional terms are defined: $\Delta U_o = U_o'' - U_o'$ in the absence of applied potential; $\Delta x_o = x_o'' - x_o'$ in the absence of applied potential.

The equations for each of the two species' potentials are the same as derived earlier (eq. 12). For the double-primed species, the total potential in the presence of a voltage over a distance, $\bar{d}$, is

$$U_{of}'' = U_o'' + \frac{z''V}{\bar{d}}(x_o'' - A) - \tfrac{1}{2}(V/\bar{d})^2(z''^2/K'') \tag{25}$$

An equivalent equation describes the singly primed species. With a voltage applied, the difference between the energy minima of the two species is

$$\Delta U_{of} - \Delta U_o = (V/\bar{d})[z''(x_o'' - A) - z'(x_o' - A)] - \tfrac{1}{2}(V/\bar{d})^2[(z''^2/K'') - (z'^2/K')] \tag{26}$$

The change in the relative positions of the wells with voltage is

$$\Delta x_{of} - \Delta x_o = (V/\bar{d})[(z'/K') - (z''/K'')] \tag{27}$$

Eqs. 26 and 27 are next discussed for four specific cases: When the force constants of the potentials are the same and different, and when the charges on each species are the same and different.

4.1. Case (a): $K'' = K'$; $z'' = z'$ $(= z)$ – congruent wells

With the substitutions as listed in the heading, eq. 27 shows that $(\Delta x_{of} - \Delta x_o) = 0$; all of the changes in the equilibrium will be due to shifts in U_o. In eq. 26, with congruent wells the term quadratic in voltage becomes zero, and

$$\Delta U_{of} - \Delta U_o = \frac{zV}{\bar{d}}\Delta x_o \tag{28}$$

The change in the equilibrium due to voltage is given by

$$\Delta U_{of} - \Delta U_o = -kT \ln[K_f/K_o] \tag{29}$$

where k is the Boltzmann constant, K_f and K_o (not to be confused with K' and K'') are the equilibrium constants in the presence and absence of the external voltage, respectively. *

Combining eqs. 28 and 29,

$$\frac{zV}{\bar{d}}\Delta x_o = -kT \ln[K_f/K_o] \tag{30}$$

If it is assumed that the charge moves through the entire applied potential – i.e., $\bar{d} \leq \Delta x_o$ – the result is the familiar Nernst equation.

$$\exp[-zV/kT] = K_f/K_o; \quad \text{for } K'' = K',\ z'' = z',\ \bar{d} \leq \Delta x_o \tag{31}$$

In the situation when z is known from independent experiments (such as an ion charge), the term $(\Delta x_o/\bar{d})$ can be determined from eq. 30. The 'fraction of the voltage traversed' is a common

* We ignore the entropy in order to relate the macroscopic equilibrium constants to the microscopic energy terms. When $z'' \neq z'$, further problems arise in accounting for activity coefficients of the differently charged species.

inference derived from the voltage dependence. With more risk, the 'distance traversed through a constant field' might be deduced.

4.2. Case (b): $K' \ll K''$; $z'' = z'$ $(= z)$ – unequal widths, fixed charge

In case a, it was seen that adjacent congruent potentials will explain Nernstian behavior. The entire voltage dependence of the equilibrium results from changes in the relative depths of the two potential wells. For congruent wells, the relative positions of the wells do not change with voltage; algebraically, $\Delta x_o \neq f(V)$. In case b, however, part of the energy of the field translates the charge distribution. This polarization energy shows up as the second term in eq. 32, which is obtained from eq. 26 using the substitutions listed in the heading.

$$\Delta U_{of} - \Delta U_o = (zV/\bar{d})\Delta x_o + \tfrac{1}{2}(V/\bar{d})^2(z^2/K') \tag{32}$$

The smaller of the two quadratic terms has been dropped.

However, it is not the partition of the energy that concerns us here, but the apparent change in equilibrium constant with a given change in voltage. We now calculate a comparison of the effects of an applied potential on the apparent equilibrium constants as calculated with the case b model followed by the two-state (Nernstian) model of case a. The following values are used: $\bar{d} = \Delta x_o = 10$ Å $= 10^{-7}$ cm, $|z| = 4$ elementary charges, $T = 285$ K, $K' = 20$ dyn cm^{-1} (representative of table 1). To keep correct units, we note that 1 eV $= 1.59 \times 10^{-12}$ erg.

The first calculation is to find $K_{\infty,f}/K_{\infty,o}$. In the absence of an applied potential, the fraction of the Gaussian distribution that lies beyond $\bar{d}$ is 0.0007 (shaded part of fig. 5). * The voltage at which $K_{\infty,f} = 0.5$ is that needed to move the broad distribution a distance $\bar{d}$ until its center coincides with the center of the narrow well. To find the needed voltage, we substitute $(\Delta x_{of} - \Delta x_o) = \bar{d}$ into equation 27, obtaining $\bar{d}^2 = Vz/K'$. From this, the voltage is calculated to be 31 mV. Thus, with a 31 mV applied potential,

$K_{\infty,f}/K_{\infty,o} = 0.5/0.0007 = 714$

For the same conditions, eq. 31, the Nernstian case, gives $K_f/K_o = 160$. The charge translation is expected to contribute the same order of voltage-dependent change in the apparent equilibrium constant. The exact values depend on the assumptions.

So far, it has been assumed that the P_{open} curve results from either one mechanism or the other: Nernstian or loosely bound charge translation. If both the Nernstian mechanism and the charge-distribution translation contribute to the P_{open} equilibrium, the following changes occur. For a curve fitted by the Nernst equation, the calculated value of $|z|$ is larger than the true value since some translation also contributes and causes the curve to be steeper. For a curve fit with a complementary error function, the force constant that is calculated is less than in reality since part of the population difference is due to changes in the relative depths of the potentials.

Finally, note that relative spatial shifts (as opposed to energy shifts) become important only when the differences between K' and K'' are great. The necessary difference in force constants and, hence, in widths can be quantified. The relative widths are found from the ratio $\sqrt{K''/K'} \approx \sqrt{2 \times 10^5/20} = 100$ as calculated for case b here. Thus, use of the sharp delineation between local (reactable) and broad (nonreactable) species seems to be reasonable. With the locally reactable widths expected to be 0.01–0.1 Å, a broad distribution is expected to be in the range 1–10 Å.

4.3. Case (c): $K' \ll K'$; $z'' = 0$, $z' \neq 0$ – unequal widths, neutralized charge

With the substitutions as listed in the heading, eq. 26 yields

$$\Delta U_{of} - \Delta U_o = (z'V/\bar{d})(x'_o - A) + \tfrac{1}{2}(V/\bar{d})^2(z'^2/K') \tag{33}$$

* The value is found as follows. The height of a normalized Gaussian at a point $\Delta x_o = \bar{d} = 10^{-7}$ cm is $0.389 \times \exp(-K'\bar{d}^2/kT)$. Upon substitution, this height is found to be 2.47×10^{-3}. A table of Gaussian properties shows that the area from $\bar{d}$ outward is 0.0007.

This special case represents the situation when the non-reactive charged group becomes electrically neutral when it transfers into the reactable species. The equation is the same as eq. 32 in form except the value of Δx_o is replaced by $(x'_o - A)$. Note that under these circumstances, the second term of the right-hand side can predominate if x'_o is close to point A. The charge translation mechanism is, thereby, enhanced.

4.4. Case (d): $K' = K''$; $z'' = 0$, $z' \neq 0$ – equal widths, neutralized charge

With the substitutions as listed, eq. 26 yields

$$\Delta U_{of} - \Delta U_o = (z'V/\bar{d})(x'_o - A) - \tfrac{1}{2}(V/\bar{d})^2(z'^2/K') \quad (34)$$

Note that eqs. 33 and 34 are identical. (An equation equivalent to eq. 34 but for $z'' \neq 0$ with $z' = 0$ results by switching superscripts.)

The expressions for the shift of $(\Delta U_{of} - \Delta U_o)$ for the unrestricted case – eq. 26 – as well as cases b–d are all of the same functional form with c and d identical. Even if the term quadratic in voltage makes no contribution, the variety of conditions which yield the same apparent voltage-dependent behavior frustrates assigning a molecular process when a Nernst equation fits the P_{open} data. From a Nernstian fit it is futile to try to ascertain whether the potential wells are congruent or not, to decide whether or not the charge involved changes in the reaction, to determine the value of the net charge, or to calculate what fraction of the voltage is traversed.

On the other hand, if it is possible to have weakly bound ionic groups present, the complementary error function is at least as likely to be correct. Such a situation is not unlikely if the charged group is attached to randomly packed polypeptide chains or chains free in solution.

Appendix A

The following is a derivation of K_∞ for charges in a square well with the dividing line between reactable and non-reactable conformations at p. The nomenclature is that of fig. 1. A potential ΔV is placed across the distance $\bar{d}$. The potential is assumed to be unaffected by the relatively dilute charges' positions.

Given the potential at a point x along the space axis is

$$V(x) = \Delta V(x/\bar{d}). \quad (A1)$$

It follows that the number density of the charged species is given by the Boltzmann distribution (degeneracies assumed unity)

$$N(x) = N_0 \exp[-\Delta V \cdot z \cdot (x/\bar{d}) \cdot \mathcal{F}/RT] \quad (A2)$$

Let

$$m = x/\bar{d} \quad (A3)$$

and

$$\zeta = -\Delta V \cdot z \cdot \mathcal{F}/RT. \quad (A4)$$

The continuum equilibrium constant is defined as the ratio of the number of molecules in configurations of the local region, B, to the number within the region ~ B.

$$[B]/[\sim B] = K_\infty = \frac{\int_p^1 e^{m\zeta}\, dm}{\int_0^p e^{m\zeta}\, dm} \quad (A5)$$

Carrying out the integration,

$$K_\infty = \frac{e^\zeta - e^{p\zeta}}{e^{p\zeta} - 1} \quad (A6)$$

Appendix B

Below is a derivation of the value of the 'factor' in the complementary error function fitting of the curve of p vs. transmembrane potential assuming it comes from a harmonically bound charged species.

By definition

$$\mathrm{erfc}(x) = \frac{2}{\sqrt{\pi}} \int_x^\infty e^{-q^2}\, dq \quad (B1)$$

We wish to relate this to the Gaussian found from the Boltzmann distribution over a harmonic potential.

The Gaussian is normalized and is given by

$$\rho(x) = (2\pi kT/K)^{-1/2} \exp\left[-\tfrac{1}{2}Kx^2/kT\right] \quad \text{(B2,16)}$$

Let

$$B = kT/K$$

Then through the substitution of $q^2 = x^2/2B$ the integral of eq. B2 is

$$(\pi)^{-1/2} \int_{(y/\sqrt{2B})}^{\infty} \exp(-q^2)\, dq = \int_y^{\infty} \rho(x)\, dx \quad \text{(B3)}$$

By comparing eqs. B1 and B3 we find

$$\tfrac{1}{2}\mathrm{erfc}(y/\sqrt{2B}) = (\pi)^{-1/2} \int_{(y/\sqrt{2B})}^{\infty} \exp(-q^2)\, dq \quad \text{(B4)}$$

By combining eqs. B3 and B4 and substituting for B, we obtain eq. 17.

$$\tfrac{1}{2}\mathrm{erfc}(y/\sqrt{2kT/K}) = \int_y^{\infty} \rho(y)\, dy \quad (17)$$

Acknowledgements

I would like to thank Gerald Alter, Richard Day, Harry Mark, Jr, Frank Meeks, and Lawrence Prochaska for making useful comments on the manuscript and during the period of development.

References

1 G.R. Freeman, J. Chem. Phys. 46 (1967) 2822.
2 G.R. Freeman, in: The study of fast processes and transient species by electron pulse radiolysis, eds. J.H. Baxendale and F. Busi (Reidel, New York, 1982) p. 19.
3 N.J.B. Green, M.J. Pilling, P. Clifford and W.G. Burns, J. Chem. Soc. Faraday Trans. I, 80 (1984) 1313.
4 R.E. Merrifield, Acc. Chem. Res. 5 (1968) 129.
5 P.W. Klymko and R. Kopelman, J. Phys. Chem. 87 (1983) 4565.
6 R.H. Conrad and L. Brand, Biochemistry 7 (1968) 777.
7 J. Yguerabide, M.A. Dillon and M. Burton, J. Chem. Phys. 40 (1964) 3040.
8 H.D. Connor, K. Shimada and M. Szwarc, Macromolecules 6 (1972) 801.
9 K. Shimada and M. Szwarc, J. Am. Chem. Soc. 97 (1975) 3313.
10 R.N. Haward, Trans. Faraday Soc. 46 (1950) 204.
11 R.D. Burkhart, J. Polym. Sci. A 3 (1965) 883.
12 M. Sisido, Macromolecules 4 (1971) 737.
13 G. Wilemski and M. Fixman, J. Chem. Phys. 60 (1974) 866.
14 P. Delahay, Double layer and electrode kinetics (Interscience, New York, 1965) part 2.
15 K.J. Laidler and M.C. King, J. Phys. Chem. 87 (1983) 2657 and references therein.
16 J.E. Hulse, R.A. Jackson and J.S. Wright, J. Chem. Ed. 51 (1974) 78.
17 J.J. Duggan and R. Grice, J. Chem. Soc. Faraday Trans. 2, 80 (1974) 795.
18 F.M. Menger, Acc. Chem. Res. 18 (1985) 128.
19 F.M. Menger, J.F. Chow, H. Kaiserman and P.C. Vasquez, J. Am. Chem. Soc. 105 (1983) 4996.
20 S. Scheiner, J. Am. Chem. Soc. 103 (1981) 315.
21 S.L. Ruby, J.C. Love, P.A. Flinn and B.J. Zabransky, Appl. Phys. Lett. 27 (1975) 320.
22 J.H. Hildebrand, Science 174 (1971) 490;
H. Ertl and F.A.L. Dullien, J. Phys. Chem. 77 (1973) 3007.
23 P.L. Fehder, C.A. Emeis and R.P. Futrelle, J. Chem. Phys. 54 (1971) 4921.
24 N.G. Van Kampen, Stochastic processes in physics and chemistry, (North-Holland, Amsterdam, 1981) ch. X.
25 H.A. Kramers, Physica 7 (1940) 284.
26 M. Doi, Chem. Phys. 9 (1975) 455.
27 R.K. Boyd, J. Chem. Phys. 60 (1974) 1214.
28 B. Widom, Science 148 (1965) 1555.
29 B. Widom, J. Chem. Phys. 55 (1971) 44.
30 B.J. Zwolinski and H. Eyring, J. Am. Chem. Soc. 69 (1947) 2702.
31 O.K. Rice, J. Phys. Chem. 65 (1961) 1972.
32 J.R. Stimers, F. Bezanilla and R.E. Taylor, J. Gen. Physiol. 85 (1985) 65.
33 R. Horn and C.A. Vandenberg, J. Gen. Physiol. 84 (1984) 505 and references therein.
34 J.R. Clay and M.F. Shlesinger, in: AIP Conference Proc. no. 109, eds. M.F. Shlesinger and B.J. West (Am. Inst. Phys. New York, 1984) p. 109.
35 H.M. Fishman, Prog. Biophys. Mol. Biol. 46 (1985) 127.
36 A.L. Hodgkin and A.F. Huxley, J. Physiol. 117 (1952) 500.
37 K.A. Rubinson, Biophys. Chem. 15 (1982) 245.
38 K.A. Rubinson, Biophys. Chem. 25 (1986) 43.
39 N. MacDonald, Time lags in biological media, (Springer-Verlag, Berlin, 1978).
40 R.E. Barker, Jr, Pure Appl. Chem. 46 (1976) 157.
41 K.A. Rubinson, Biophys. Chem. 12 (1980) 51.
42 H.J.V. Tyrrell and K.R. Harris, Diffusion in liquids (Butterworths, London, 1984) ch. 6.
43 P.N.T. Unwin and P.D. Ennis, Nature 307 (1984) 609.
44 L. Hellemans and M. De Maeyer, J. Chem. Soc. Faraday Trans. 2, 78 (1982) 401.
45 R.L. Barchi, J. Neurochem. 40 (1983) 1377.
46 T. Narahashi, Physiol. Rev. 54 (1974) 813.
47 M. Noda, S. Shimizu, T. Tanabe, T. Takai, T. Kayano, T. Ikeda, H. Takahashi, H. Nakayama, Y. Kanaoka, N.

Minamino, K. Kangawa, H. Matsuo, M.A. Raftery, T. Hirose, S. Inayama, H. Hayashida, T. Miyata and S. Numa, Nature 312 (1984) 121.
48 E. Moczydlowski, S. Garber and C. Miller, J. Gen. Physiol. 84 (1984) 665.
49 H. Frohlich, Proc. Natl. Acad. Sci. U.S.A. 72 (1975) 4211.
50 K.D. Moller and W.G. Rothschild, Far infrared spectroscopy (Wiley-Interscience, New York, 1971).
51 P.C. Painter, M.M. Coleman and J.L. Koenig, The theory of vibrational spectroscopy and its application to polymeric materials (Wiley-Interscience, New York, 1982).
52 M. Reiner, Deformation, strain, and flow (H.K. Lewis, London, 1969).
53 T. Alfrey, Jr, Mechanical behavior of high polymers (Interscience, New York, 1948) p. 434.
54 L.E. Peterson, R.L. Anthony and E. Guth, Indust. Eng. Chem. 34 (1942) 1349.
55 M.F. Muller and J.D. Ferry, Biopolymers 23 (1984) 2311.
56 W. Kuhn, Kolloid Z. 68 (1934) 2.
57 F.T. Wall, J. Chem. Phys. 11 (1943) 527.
58 L.R.G. Treloar, Trans. Faraday Soc. 39 (1943) 36.
59 C.M. Armstrong, F. Bezanilla and E. Rojas, J. Gen. Physiol. 62 (1973) 375.
60 E. Rojas and B. Rudy, J. Physiol. 262 (1976) 501.
61 G.K. Wang, J. Physiol. 346 (1984) 127 and references therein.
62 G.W. Koeppl and A.J. Kresge, J. Chem. Soc. Chem. Commun. (1973) 371.
63 M.M. Bonnemay, C.R. Acad. Sci. 223 (1946) 76.
64 R. Audubert, Disc. Faraday Soc. 1 (1947) 72.
65 M. Polanyi, Acta Physiochim. 2 (1935) 505.